

Mechanisms of the Breakup of Liquid Jets

S. P. Lin* and Z. W. Lian†

Clarkson University, Potsdam, New York

A general theory of the onset of breakup of liquid jets in an ambient gas is given. The theory is based on the linear stability analysis of a viscous liquid jet with respect to spatially growing disturbances. The three independent parameters in the theory are the Reynolds number R , the Weber number We , and the gas-to-liquid density ratio Q . The numerical results obtained from a single characteristic equation over a wide range of the parameter space reveal that there are two fundamentally different mechanisms of the jet breakup. The first is the capillary pinching that breaks up the jet into segments. The second is the capillary wave resonance with the gas pressure fluctuation that generates droplets much smaller than the jet diameter. An argument based on the boundary-layer instability theory is used to demonstrate that the shear waves at the liquid-gas interface plays a secondary role in the jet breakup.

Introduction

ATOMIZATION is a process of breaking up a jet into droplets of diameter much smaller than the jet diameter. This process is widely used in industrial applications including fuel injections in internal combustion engines. A good knowledge of the fundamental mechanism of atomization is essential for raising the combustion efficiency and reducing the environmental pollution. Unfortunately our understanding of the fundamental mechanism is far from complete. This work delineates the parameter range of operation in which atomization can be achieved. Distinctive mechanisms of jet breakup in the atomization regime as well as other regimes are elucidated.

Plateau¹ observed that the surface energy of a uniform circular cylindrical jet is not the minimum attainable for a given jet volume. He argued that the jet tends to break up into equal segments of length, which is nine times the jet radius, because the spherical droplets formed from these segments give the minimum surface energy for the same jet volume. Neglecting the effects of gravity and ambient gas, Rayleigh² showed that the mechanism of the jet breakup is the hydrodynamic instability caused by the surface tension. He introduced into the jet infinitesimal disturbances that may grow or decay everywhere in the jet at the same rate. He found that the fastest growing disturbance has a wavelength equaling nine times the jet radius. Weber³ and Chandrasekhar⁴ found that the viscosity has only a stabilizing effect that reduces the breakup rate and increases the drop size. Keller et al.⁵ observed that these theories were based on the assumption that the disturbances are temporally growing, while the observed disturbances actually grow in space in the flow direction. In particular, the disturbance at the nozzle exit cannot grow in time. They extended Rayleigh's analysis for spatially growing disturbances and found that Rayleigh's results are relevant only to the case of small values of the Weber number, which is the ratio of the surface tension force to the liquid inertia force. For the Weber number of order one or greater, they found a new mode of faster growing disturbances of much larger wavelengths than those of the Rayleigh mode. An association of this mode with the absolute instability was made by Leib and Goldstein.^{6,7} Note that in the above-mentioned theories, the effect of the ambient gas is neglected, and

that the predicted drop sizes are of the same order as the jet diameter. Thus, these theories cannot be applied to the atomization phenomenon, which is the breakup of a liquid jet into droplets much smaller than the jet diameter. To explain the atomization process, Taylor⁸ took the gas density into account. He considered the limiting case of an infinitely thick jet and extremely small gas-to-liquid density ratio. Taylor's analysis for the case of temporally growing disturbances with small density ratios was extended by Lin and Kang⁹ to the case of spatially growing disturbances with finite density ratios. Lin and Kang showed that the spray angle is proportional to the imaginary part of the complex wave number corresponding to the fastest growing disturbances. They compared the predicted drop sizes caused by the pressure fluctuation and by the shear waves at the liquid-gas interface with the experiments of Reitz and Bracco¹⁰ and concluded that the basic mechanism of atomization is the interfacial instability caused by the pressure fluctuation. Lin and Kang also discussed the relationship between temporally and spatially growing disturbances. Their results showed that the maximum growth rates of disturbances all occur at wave numbers of order one in the parameter range relevant to atomization. The drop size being proportional to the wavelength and the wavelength being normalized by the capillary length, the atomized droplet diameters are therefore proportional to the capillary length a , which is the ratio of surface tension to the inertia force per unit volume of the ambient gas; i.e., $\sigma/\rho_2 U^2$, where σ is the surface tension, ρ_2 is the gas density, and U is the jet speed. Since the atomized droplets are much smaller than the jet radius r_o , we must have

$$a/r_o = \sigma/(\rho_1 U^2 r_o)(\rho_1/\rho_2) = We(\rho_1/\rho_2) \ll 1 \quad (1)$$

where ρ_1 is the liquid density. It follows from Eq. (1) that the necessary condition for atomization is $We \ll Q$, where $Q = \rho_2/\rho_1$. The work of Lin and Kang⁹ covered only this atomization regime. Consequently, they were unable to delineate both Taylor's atomization regime and Rayleigh's capillary pinching regime in the same parameter space. This delineation is done here for the first time with the aid of numerical results obtained from the same characteristic equation. This enables us to gain a more unified understanding of the mechanism of jet breakup. It follows from the definition of a that we must have for the Rayleigh regime $a/r_o = We/Q > 1$, since Rayleigh's capillary pinching results in droplets of diameters larger than the jet diameter. The effect of the Reynolds number on this regime is expounded in this work. Efforts to gain a unified understanding of the mechanism of jet breakup are well documented.^{11,12} Although the previous works were based on various asymptotic analysis of tempo-

Received June 20, 1988; revision received Dec. 9, 1988. Copyright © 1988 American Institute of Aeronautics and Astronautics, Inc. All rights reserved.

*Professor, Department of Mechanical and Industrial Engineering.

†Graduate Student, Department of Mechanical and Industrial Engineering.

Fig. 1 The Rayleigh and Taylor modes.

In the limiting case of $Q \rightarrow 0$, after using the equation preceding Eq. (3), Eq. (2) is reduced to

$$2k^2(k^2 + \lambda^2) \cdot \frac{I_1'(k)}{I_0(k)} \left[1 - \frac{2k\lambda}{k^2 + \lambda^2} \cdot \frac{I_1(k)I_1'(\lambda)}{I_1(\lambda)I_1'(k)} \right] - (k^4 - \lambda^4) - (1 - k^2)Jk \frac{I_1(k)}{I_0(k)} = 0 \quad (7)$$

where $J = R^2 We$. This is the characteristic equation given by Chandrasekhar⁴ for the breakup of viscous liquid threads in vacuum.

In the Taylor limit $r_o \rightarrow \infty$, k in Eq. (1) can be rescaled with the capillary length a as

$$k = Ka(r_o/a) \equiv \bar{k}(\bar{r}_o/a), \quad K = 2\pi/\text{wavelength}$$

where K is the dimensional wave number. Note that $k \rightarrow \infty$ needs not imply that $\bar{k} \rightarrow \infty$. In fact Taylor's results show that $\bar{k} = \mathcal{O}(1)$. By use of asymptotic expansions of the Bessel functions for $k \rightarrow \infty$ as $(r_o/a) \rightarrow \infty$, we reduce Eq. (2) to

$$[R(\omega - ik) + 2k^2]^2 + R^2 We k^3 + QR^2 \omega^2 - 4k^2 \lambda = 0 \quad (8)$$

This is the equation obtained by Taylor⁸, see Lin and Kang.⁹ Note that $(r_o/a) \rightarrow \infty$ implies $R \rightarrow \infty$, and by virtue of Eq. (1) $We/Q \rightarrow 0$. The growth rate curve obtained from Eq. (8) with $\omega = i\omega_i$ for the values of $R = 2 \times 10^4$, $We = 1.964 \times 10^{-5}$ and $Q = 0.0013$ is plotted as curve T in Fig. 1. The curve right below curve T is obtained from Eq. (2) for the same parameters. Lin and Kang showed that when $Q \ll 0.01$, Taylor's temporal growth rate is related to the spatial growth rate of Lin and Kang by the Gaster¹⁷ theorem. However, when the density ratio is of order 10^{-2} or greater, the spatial and temporal theories differ significantly.

The rest of the paper will be devoted to the elucidation of the breakup of viscous liquid jets of finite radius in the gas by use of hitherto unavailable results. The results are obtained from the solution of Eq. (2) over a wide range of the relevant parameters We , R , and Q . The method of solution used is the Muller method.¹⁸ Since the observed disturbances grow spatially and oscillate temporally in atomization, we treat ω as purely imaginary but k as complex, i.e., $\omega = i\omega_i$ and $k = k_r + ik_i$. Here we do not consider the case of absolute instability for which the disturbance grows both spatially and temporally.¹⁴

The solution of the equation obtained by Keller et al. for the case of $R = \infty$, $Q = 0$, and $We = 0.0025$ is reproduced as curve R in Fig. 2. For the same values of $We = 0.0025$ and $R = 2 \times 10^4$, two additional curves in the same figure are obtained from Eq. (2), respectively, with $Q = 10^4$ and $Q = 0.0013$. The value of $Q = 0.0013$ corresponds to the air-to-water density ratio in one atmosphere at room temperature. It is seen that the presence of the atmosphere tends to increase the maximum amplification rate by more than 20% over that predicted by the Rayleigh equation (3). This deviation is even greater either when Q becomes greater or R becomes smaller. Hence, Rayleigh's results are good approximations if $Q < 0.0013$ and $R > 10^4$. The experimental results of Goedde and Yuen¹⁹ and Donnelly and Glaberson²⁰ are included in the same figure for comparisons. Their experiments were conducted at one atmospheric pressure and room temperature. They did not record the values of R and We for each of the experimental points, since their experiments were intended for comparisons with Rayleigh's theory, which is independent of the jet velocity. However, the ranges of R and We can be calculated from their experimental data to be $(3 \sim 10) \times 10^3$ and $(1.44 \sim 8) \times 10^{-3}$, respectively. Note that the values of We used for the theoretical curve in Fig. 2 are of the same orders as those in the experiments. However, the values of R used for the plots including Rayleigh's curve are larger than the experimental values. Note that the temporal

growth rate $\omega/(\sigma/r_o^3 \rho_1)^{1/2} \equiv \omega'$ reported by Goedde and Yuen is related to k_i through Eq. (6) by $k_i = \omega_{Ri} = We^{1/2} \omega'$, because of different nondimensionalizations used. It appears that the results of experiments in the atmosphere agree better with the theory of the inviscid jet breakup in a vacuum rather than with the corresponding theory of breakup of a viscous jet in atmosphere. The better agreement is probably fortuitous. The growth rates at the swell and the neck in the experiments were found to be different constants. The growth rate was taken to be the logarithm of the difference between those at the neck and the swell in the jet. This is neither consistent with the temporal growth rate which is theoretically the same constant everywhere in the jet nor is it consistent with the definition of spatial growth rate. Thus, the comparisons were made between two physically different quantities. New measurements of spatial growth rates as functions of R , We , and Q are very desirable. Two amplification curves for two different values of We are plotted near curve R in Fig. 3 for $Q = 0.0013$ and $R = 2 \times 10^4$. The curve R is the same curve R given in Fig. 1. The amplification rate increases as We is increased, clearly indicating that surface tension is the destabilizing factor. The jet axial velocity relaxation was shown by Leib and Goldstein⁶ to make the Rayleigh mode more unstable. However, the mechanism remains the capillary pinching.

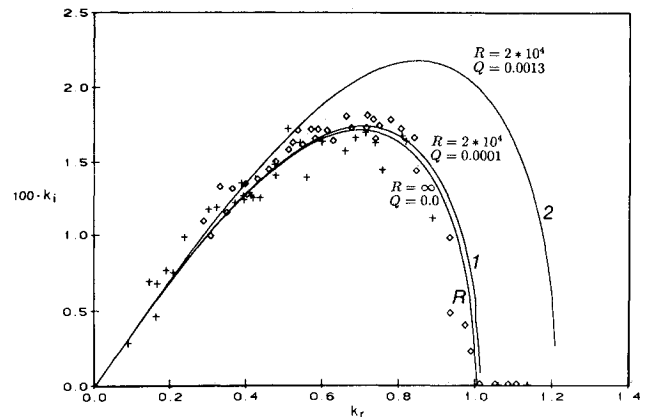


Fig. 2 Ambient gas is destabilizing in the Rayleigh mode; $We = 0.0025$. +: experiments of Goedde and Yuen. \diamond : experiments of Donnelly and Glaberson.

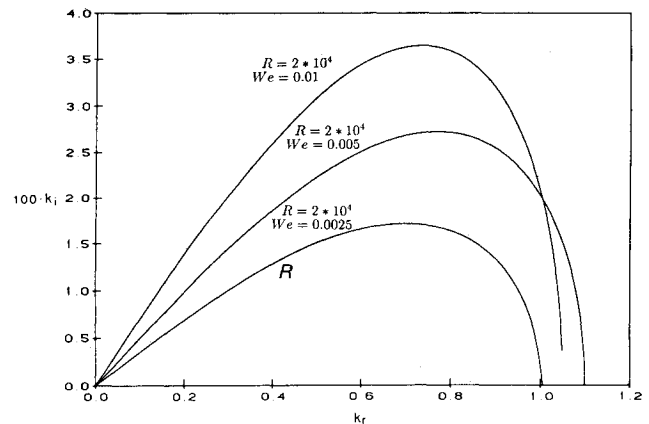


Fig. 3 Capillary pinching in the Rayleigh mode ($Q = 0.0013$).

On the contrary, surface tension is a stabilizing factor for the Taylor mode. This is seen from the three curves plotted near curves T of Fig. 4 for three different values of We . The curve T is the same curve T appearing in Fig. 1. As We is increased with $R = 2 \times 10^4$ and $Q = 0.0013$ held constant, we see that the amplification is decreased. Thus, the major difference between the jet breakup by the Rayleigh mode and by the Taylor mode is that, while the former is due to capillary pinching,⁵ the latter is due to a mean other than surface tension, because surface tension is stabilizing. This other mean is either due to the pressure fluctuation or shear stress at the interface. The interfacial shear will be eliminated as the cause of atomization on physical grounds. The factors involved in the nozzle are excluded, because the site of atomization is at the interface. These factors can affect the atomization only indirectly.⁹ Note that $We = 2.5 \times 10^{-3} \sim 10^{-2}$ for the Rayleigh mode, and $We = 2 \times 10^{-4} \sim 2 \times 10^{-6}$ for the Taylor mode at $Q = 0.0013$ and $R = 2 \times 10^4$. Hence, there is a value of We between 10^{-3} and 10^{-4} below which the breakup is due to pressure fluctuation but above which it is due to the capillary pinching. The specific turn-around value of We depends on the values of R and Q given, and will be further explained later.

The curves A in Fig. 5 is the amplification curve for $R = 34.5$, $Q = 0.0013$, and $We = 0.0025$. The curve S is obtained from Eq. (7) with the same values of We and R but for $Q = 0$. The ambient gas is again destabilizing. The corresponding experimental results of Goedde and Yuen¹⁹ are also presented for comparison. The measured growth rate ω for this case was normalized by (v/r_o^2) . Thus, their growth rate is related to our k_i through Eq. (6), and is given by

$$k_i = \omega_{Ri} = \omega/(v/r_o^2)R$$

The two additional curves in Fig. 5 for two different values of We and $Q = 0$ show that, when compared with the Rayleigh modes depicted in Fig. 1, the surface tension remains a destabilizing factor even if the liquid viscosity is increased to reduce R to 34.5. Note that in the case of $Q = 0$, the only relevant parameter is $J = R^2 We$. Thus, the curve S in Fig. 5 can be used for any R and We as long as the corresponding J remains 2.976. This fact will be used to show that the nonvanishing of Q is essential for the Taylor mode. Consider the curve with $Q = 0.0013$, $We = 0.744 \times 10^{-8}$, and $R = 2 \times 10^4$ belonging to the Taylor atomization regime in Fig. 1. Retaining the same values of We and R but putting $Q = 0$, we obtain an amplification curve that is exactly the curve S given in Fig. 5 since the value of J remains 2.976. Thus, the curve in the Taylor regime is brought down to the Rayleigh regime simply by reducing the values of Q from 0.0013 to 0. Hence, in order to remain in the atomization regime, the presence of ambient gas is essential. Without the ambient gas, atomization cannot occur even if the surface tension is so small that $We = 0.744 \times 10^{-8}$.

Figure 6 shows that even when R is reduced to 0.1 the breakup mechanism remains the capillary pinching when $We > Q$, since the amplification rate increases with We .

The amplification curves for $We = 1.964 \times 10^{-5}$, $R = 3.371 \times 10^4$, and two different values of Q given in Fig. 7 together with the curve for the same values of We and R but with $Q = 0.0013$ given in Fig. 1 show how the amplification rate and the range of unstable wavelengths of the Taylor mode are increased as Q is increased from 0.0013 to 0.13. This range of Q corresponds to the air-to-water density ratio under pressure ranging from 1–100 atmospheric pressure. The same destabilizing effect of Q for the Rayleigh mode is depicted in the lower left corner of Fig. 1. Figures 8 and 9 show the damping effect of viscosity on the Rayleigh and Taylor modes.

The present theory can be used to explain the spray angle θ of an atomizing jet. The displacement of the interface from its unperturbed position is $d = C_o \exp[i(\omega_i \tau + k z)]$, where C_o is

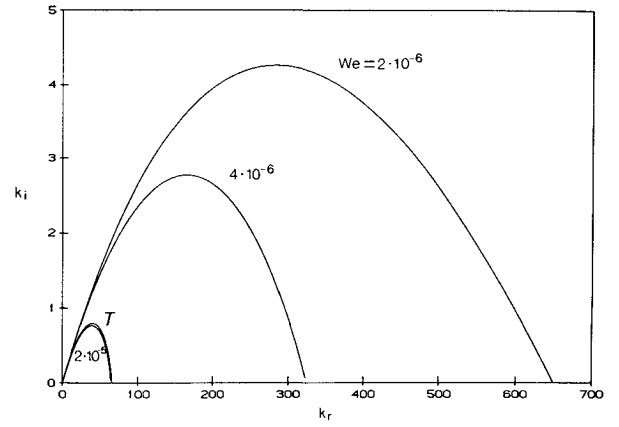


Fig. 4 Surface tension is stabilizing in the Taylor mode ($R = 2 \times 10^4$, $Q = 0.0013$).

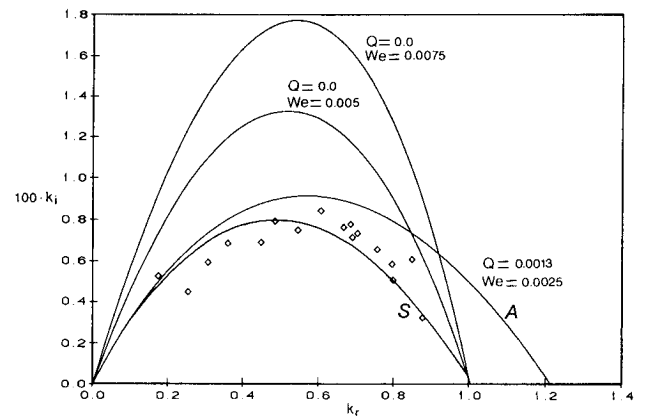


Fig. 5 Ambient gas and surface tension are destabilizing in the viscous Rayleigh jet, $R = 34.5$. \diamond : experiments of Goedde and Yuen.

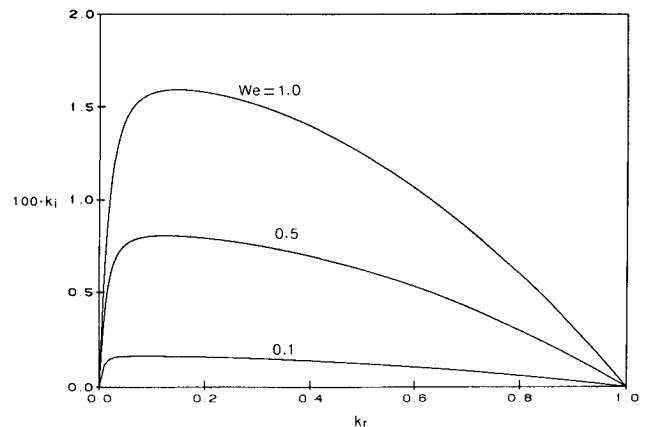


Fig. 6 Surface tension is destabilizing in a very viscous thread ($R = 0.1$, $Q = 0.001$).

the initial amplitude at the nozzle exit, which remains arbitrary in the linear theory. Thus,

$$\tan(\theta/2) = -\frac{d}{dy}(\text{envelope of } d) = C_o k_i \exp(-k_i y) \quad (9)$$

Expanding Eq. (9) in Taylor's series, we have

$$\tan(\theta/2) = C_o k_i (1 - k_i y + \dots) \quad (10)$$

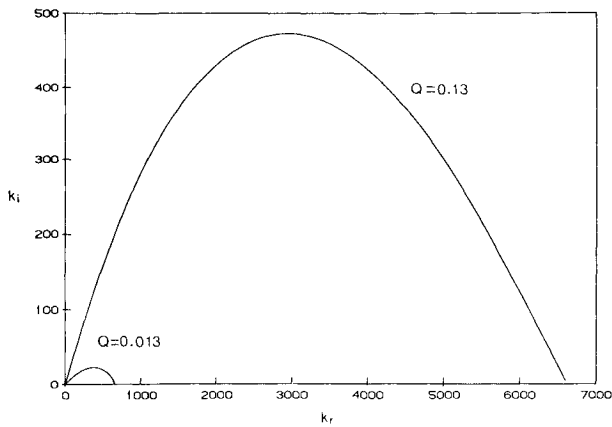


Fig. 7 Destabilizing effects of the ambient gas in the Taylor mode ($We = 1.964 \times 10^{-5}$, $R = 33705$).

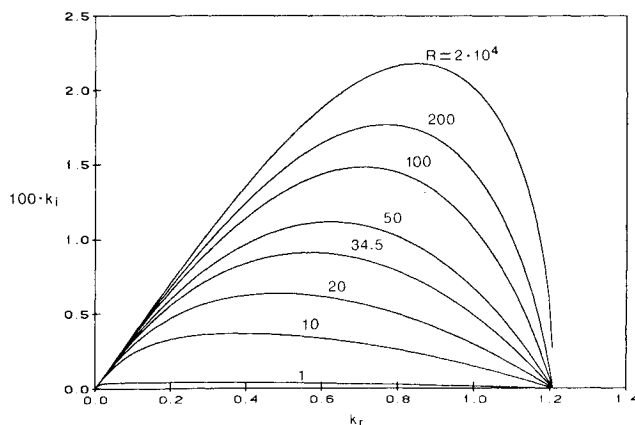


Fig. 8 Viscous damping of the Rayleigh mode in the presence of ambient gas ($We = 0.0025$, $Q = 0.0013$).

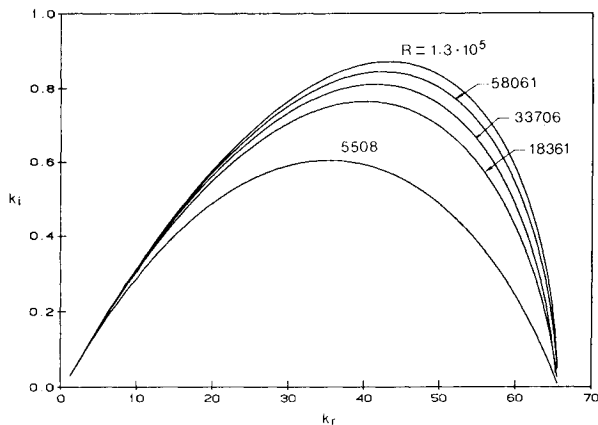


Fig. 9 Viscous damping of the Taylor mode ($We = 1.964 \times 10^{-5}$, $Q = 0.0013$).

Hence, unless $C_o k_i$ is sufficiently large, a measureable θ may not appear until some distance downstream in the $-y$ direction. This may be the origin of the so-called intact length over which the jet does not appear to diverge. Table 1 compares the spray angles θ measured by Reitz and Bracco¹⁰ in their test series 64–67 with that predicted with the present theory. Tangent of half of the measured spray angles, i.e., $\tan(\theta/2)$, are given in the fourth column of Table 1. The predicted values of k_i , which is related to spray angle by Eq. (10), are given in the seventh column of the same table. When the measured values of $\tan(\theta/2)$ are substituted into the left side of Eq. (10), and the predicted values of k_i are substituted into the right side of Eq. (10), it is found that at the nozzle exit where $y = 0$ this equation is satisfied only if the values of the coefficients C_o are given by that given in the sixth column of Table 1. C_o represents the initial disturbance amplitude at the nozzle exit. It appears that the spray angles depend not only on the spatial growth rate k_i but also on the initial disturbance amplitude C_o at the nozzle exit. Note that these values of C_o are all of the same order of magnitude, probably reflecting the fact that the level of disturbances at the nozzle exit in the different series of tests are about the same. A full nonlinear theory is required to make a quantitative statement, however.

Discussion

The results for some limiting cases of the unified theory and their comparisons with some limited experimental results have been used to demonstrate the validity and the limitations of the theories of Rayleigh, Weber, Chandrasekhar, Taylor, and Keller et al. on the onset of the liquid jet breakup. However, it was assumed that the viscosity of gas is of secondary importance in the process. This assumption must be examined. If the viscosity is present in the ambient gas, the high speed of the liquid jet will cause the formation of a thin boundary layer near the liquid–gas interface. The boundary layer may become unstable and generate the Tollmein–Schlichting²¹ waves (shear waves). The shear waves may extract kinetic energy from the mean flow and amplify. Thus, the shear waves may participate with the pressure fluctuation and capillary force in bringing about the breakup of liquid jets. The order of magnitude of the size of droplets generated by the shear waves may be estimated with the critical shear wavelength at the onset of the boundary-layer instability. The velocity profile in the boundary layer near the free surface of a jet is not known. The boundary layer flows, over continuously moving solid surfaces in an otherwise quiescent fluid,^{22–24} are probably the closest known flows to the free surface boundary-layer flows. Unfortunately, the stability results of these flows are not available. For this reason, we will use the stability results for the Blasius flow²¹ over a stationary solid surface to estimate the size of droplets generated by shear waves. It should be pointed out that the shear stress and the velocity distributions in both types of solid surface boundary layers are of the same order of magnitude. Therefore, we do not expect to obtain a different order of magnitude of drop size from a “solid jet” boundary-layer flow even if the stability results of this flow are available. The critical Reynolds number and the critical wavelength of the Blasius

Table 1 Spray angles of atomizing jets

Series	$Q \times 10^3$	$We \times 10^5$	r_o/a	$\tan(\theta/2) \times 10^2$	C_o	$k_i \times 10^2$	$a \times 10^5$ cm
64	1.3	2.754	944	1.66	0.6	2.77	36.02
65	7.7	2.754	559	8.31	1.43	5.81	6.08
66	25.8	2.504	2061	16.46	2.13	7.73	1.65
67	51.5	2.527	4096	14.95	2.60	5.75	0.83

Table 2 Onset of jet breakup

Mechanism	Characteristic length	Parameter range (mode)
		$R > 10^4$ (Rayleigh)
Capillary pinching	r_o	$Q \ll We$
		$R < 10^4$ (Weber–Chandrasekhar)
Pressure Fluctuation	$a = (We/Q)r_o$	$We \ll Q < 1$, $Q < We$
		$1 \leq R$ (Taylor) $R \sim 26180(v_2/v_1)$
Shear waves	$\lambda_c = 26180r_o(v_2/v_1)/R$	$Q > We$
		$R \sim 26180(v_2/v_1)(Q/We)$

profile are given, respectively, by²⁵

$$R_c = U\delta/v_2 = 400, \quad \lambda_c = (2\pi/0.3)(\delta/0.32) \quad (11)$$

It follows from Eq. (11) that

$$\lambda_c = 26180 v_2/U \quad (12)$$

Thus, in general, there are three length scales λ_c , r_o , and a characterizing the size of droplets caused by shear waves, capillary pinching, and the pressure fluctuation, respectively. Depending on the range of parameters, one or two characteristic lengths may be predominant.

For example, consider a jet of 0.034-cm diameter with a maximum velocity of 1.11×10^4 cm/s. This is the water jet atomized under 1 atm in test 23 of Reitz and Bracco.¹⁰ Using $v_2 = 0.15$ cm²/s at room temperature, we find from Eq. (11) that $\lambda_c = 0.35$ cm. Using $v_1 = 0.01$ cm³/s, $\sigma = 72$ dynes/cm, $\rho_1 = 1$ g/cm³, $\rho_2 = 0.0013$ g/cm³, we find $R = 18870$, $We = 3.438 \times 10^{-5}$, and $Q = 1.3 \times 10^{-3}$. Thus, the present jet is operating in the Taylor regime since $We \ll Q$, and the characteristic wavelength is $2\pi a = 2.8 \times 10^{-3}$ cm. This is several orders of magnitude smaller than λ_c and $2\pi r_o = 0.11$ cm. Therefore, in the process of atomizing this jet, the shear waves play little role, since the measured atomized droplets scale with a .

If both the diameter and the velocity of the jet in the last example is reduced by a factor of 10, we have $R = 188.7$, $We = 3.438 \times 10^{-2}$, and $Q = 1.3 \times 10^{-3}$. Thus, $We \gg Q$ and the jet is now operated well within the Rayleigh regime although the damping effect of the liquid viscosity neglected by Rayleigh is now significant at $R = 188.7$. The characteristic length is of order $2\pi r_o = 0.011$ cm, which is two orders of magnitude smaller than the critical shear wavelength $\lambda_c = 3.5$ cm and one order of magnitude smaller than $2\pi a = 0.28$ cm. Hence, the shear wave and the pressure fluctuation are not responsible for the breakup. The breakup in the Rayleigh regime is by the capillary pinching.

We conclude by reiterating that there are three characteristic lengths in the jet breakup. They are relevant to three distinctive mechanisms that operate in different parameter ranges. These are summarized in Table 2. However, it can be seen from this table that a jet may actually breakup by more than one mechanism in the overlap regions of the characteristic parameter space. For example, it may break up under the simultaneous actions of the capillary pinching and the pressure fluctuation. This occurs when $We/Q = \mathcal{O}(1)$. Consider a water jet of 0.034-cm diameter issued at 1.11×10^3 cm/s into the atmosphere at room temperature. The relevant parameters are $R = 1887$, $We = 3.438 \times 10^{-3}$, and $Q = 0.0013$. Then $We \sim Q$, and the jet is broken up at the outer edge of the Rayleigh regime discussed in the previous section. The characteristic wavelength is now of the order of $2\pi r_o = 0.11$ cm, which is of the same order as the atomization length $2\pi a = 0.28$ cm, but much smaller than the possible shear

wavelength $\lambda_c = 3.5$ cm. Therefore the shear wave is again a bystander of the event of the breakup. However, the breakup is now under the simultaneous actions of the capillary pinching and the pressure fluctuation which may, in general, produce a bimodal distribution of the drop sizes. In order to enable the shear waves to assist significantly the capillary pinching in the breakup process, we must have $r_o \sim \lambda_c$, and $We > Q$. It follows from Eq. (12) that this requires

$$\sigma > (26180.v_2)^2 \rho_2 / r_o$$

For the sake of demonstration, let $v_2 = 0.15$ cm² and $\sigma = 72$ dynes/cm. Then the above inequality becomes

$$(\rho_2/r_o) < 4.67 \times 10^{-6} \text{ g/cm}^4$$

This condition is difficult to satisfy in common practice for gases in 1 atm. However, for a water jet of 0.35-cm radius and $U = 3 \times 10^3$ cm/s in a rarefied gas of $\rho_2 = 10^{-6}$ g/cm³, we have $We = 2.29 \times 10^{-5} > Q = 10^{-6}$, $R = 105000$, $\lambda_c = 1.31$ cm, $2\pi r_o = 2.1$ cm, and the above inequality is satisfied. Only when the density of the gas is reduced to such a low level can the capillary pinching and the interfacial shear work hand in hand without the interference from the pressure fluctuation. Finally, in order to induce the shear waves to assist the atomization, we require $\lambda_c \sim a$ and $We < Q$, i.e.,

$$\sigma \sim 26180 \rho_2 v_2 U, \quad \sigma < \rho_2 U^2 r_o$$

Using $v_2 = 0.15$ cm²/s, we can combine the above two relations to give

$$4.668 \times 10^{-6} \text{ g/cm}^4 > \rho_2 / r_o$$

Again, this condition can be satisfied only in a very low-density gas and by a relatively thick jet. Thus, for example, if $\rho_2 = 10^{-5}$ g/cm³, $\rho_1 = 1$ g/cm³, $\sigma = 72$ dynes/cm, $v_2 = 0.15$ cm²/s, $r_o = 10$ cm, and $U = 3000$ cm/s, we have $R = 3 \times 10^6$, $We = 0.8 \times 10^{-6} < 10^{-5}$, $\lambda_c = 1.31$ cm, $a = 1.8$ cm, and the required condition is satisfied. This example demonstrates how hard it is to induce the shear wave to assist in the onset of atomization. It should be emphasized that we are referring here to the role of the shear waves on the onset of atomization. Obviously, in a fully turbulent gas the atomization process may be assisted by the small part of turbulence spectrum whose wavelengths are of the same order of magnitude as the capillary length a . It should also be pointed out that the gas viscosity is treated as a parameter in this analysis. A more precise delineation of the breakup regimes can be achieved by a more complete stability analysis that considers the coupled effects of the gas viscosity with all other relevant physical properties. A nonlinear theory of atomization of a viscous liquid jet in a viscous gas is not yet available.²⁶

Acknowledgment

This work was supported in part by Grant DAAL03-86-K-0072 of the Army Research Office, Grant MSM-8817372 of National Science Foundation, and a New York State Science and Technology Grant. The numerical computation was carried out with the Cornell National Supercomputer Facility at Cornell University, which is funded in part by NSF, New York State, and IBM.

References

- ¹Plateau, J., *Statique Experimentale Et Theorie Des Liquids Sou-mie Aux Seules Forces Moleculaires*, Canthier Vallars, Paris, 1873.
- ²Rayleigh, L., "On the Instability of Jets," *London Mathematical Society*, Vol. 10, 1879, pp. 361–371.
- ³Weber, C. Z., "Zum Zerfall eines Flussigkeitsstrahles," *Mathe-matik and Mechanik*, Vol. 11, April 1931, pp. 136–154.
- ⁴Chandrasekhar, S., *Hydrodynamic and Hydromagnetic Stability*, Oxford University Press, Oxford, England, 1961, p. 537.
- ⁵Keller, J. B., Rubinow, S. I., and Tu, Y. O., "Spatial Instability of a Jet," *Physics of Fluids*, Vol. 16, Dec. 1972, pp. 2052–2055.
- ⁶Leib, S. J. and Goldstein, M. E., "The Generation of Capillary Instabilities on a Liquid Jet," *Journal of Fluid Mechanics*, Vol. 168, 1986, pp. 479–500.
- ⁷Leib, S. J. and Goldstein, M. E., "Convective and Absolute Instability of a Viscous Liquid Jet," *Physics of Fluids*, Vol. 29, April 1986, pp. 952–954.
- ⁸Taylor, G. I., "Generation of Ripples by Wind Blowing Over Viscous Fluids," *The Scientific Papers of G. I. Taylor*, Cambridge University Press, Cambridge, England 1963, Vol. 3, pp. 244–254.
- ⁹Lin, S. P. and Kang, D. J., "Atomization of a Liquid Jet," *Physics of Fluids*, Vol. 30, July 1987, pp. 2000–2006.
- ¹⁰Reitz, R. D. and Bracco, F. V., "Mechanism of Atomization of a Liquid Jet," *Physics of Fluids*, Vol. 25, 1982, pp. 1730–1742.
- ¹¹Reitz, R. D. and Bracco, F. V., "Mechanisms of Breakup of Round Liquid Jets," *Encyclopedia of Fluid Mechanics*, Vol. 3, edited by N. P. Cheremisinoff, Gulf P. Houston, 1986, pp. 233–249.
- ¹²Reitz, R. D., "Modeling Atomization Processes in High-Pressure Sprays," *Atomization and Spray Technology*, Vol. 4, 1988, pp. (to appear).
- ¹³Sterling, A. M. and Sleicher, C. A., "Stability of Capillary Jets," *Journal of Fluid Mechanics*, Vol. 68, 1975, pp. 477–495.
- ¹⁴Lin, S. P. and Lian, Z. W., "Absolute Instability of a Liquid Jet in a Gas," *Physics of Fluids*, Vol. 32, March 1989, pp. 490–499.
- ¹⁵Lin, S. P., "Stability of a Viscous Liquid Curtain," *Journal of Fluid Mechanics*, Vol. 104, 1981, p. 111–118.
- ¹⁶Lin, S. P., "Waves in a Viscous Liquid Curtain," *Journal of Fluid Mechanics*, Vol. 112, 1981, pp. 443–458.
- ¹⁷Gaster, M., "A Note on the Relation Between Temporally In-creasing and Spatially Increasing Disturbances in Hydrodynamic Stability," *Journal of Fluid Mechanics*, Vol. 14, 1962, pp. 222–224.
- ¹⁸Muller, D. E., "A Method for Solving Algebraic Equations Using an Automatic Computer," *Mathematical Tables and Aids to Compu-tation*, Vol. 10, 1956, pp. 208–230.
- ¹⁹Goedde, E. F. and Yuen, M. C., "Experiments on Liquid Jet Instability," *Journal of Fluid Mechanics*, Vol. 40, 1970, pp. 495–512.
- ²⁰Donnelly, R. J. and Glaberson, W., "Experiments on the Capil-lary Instability of a Liquid Jet," *Proceedings of the Royal Society*, London, Vol. 290, pp. 547–556.
- ²¹Schlichting, H., *Boundary-Layer Theory*, McGraw-Hill, New York, 1968, p. 447.
- ²²Sakiadis, B. C., "Boundary-Layer Behavior on Continuous Solid Surfaces: III. The Boundary Layer on a Continuous Cylindrical Surface," *AIChE Journal*, Vol. 7, 1961, pp. 467–472.
- ²³Koldenhof, E. A., "Laminar Boundary Layers on Continuous Flat and Cylindrical Surface," *AIChE Journal*, Vol. 9, 1963, pp. 411–418.
- ²⁴Tsou, F. K., Sparrow, E. M., and Goldstein, R. J., "Flow and Heat Transfer in the Boundary Layer on a Continuous Moving Surface," *International Journal of Heat and Mass Transfer*, Vol. 10, 1967, pp. 219–235.
- ²⁵Drazin, P. G. and Reid, W. H., *Hydrodynamic Stability*, Cam-bridge University Press, Cambridge, England 1981, p. 224.
- ²⁶Bogy, D. B., "Drop Formation in a Circular Liquid Jet," *Annual Review of Fluid Mechanics*, Vol. 11, 1979, pp. 207–228.